International Journal of Mechanical, Industrial and Aerospace Sciences
ISSN: 2517-9950
Vol:7, No:7, 2013

# Analysis of Flow in Cylindrical Mixing Chamber

Václav Dvořák

***Abstract*—**The article deals with numerical investigation of axi-symmetric subsonic air to air ejector. An analysis of flow and mixing processes in cylindrical mixing chamber are made. Several modes with different velocity and ejection ratio are presented. The mixing processes are described and differences between flow in the initial region of mixing and the main region of mixing are described. The lengths of both regions are evaluated. Transition point and point where the mixing processes are finished are identified. It was found that the length of the initial region of mixing is strongly dependent on the velocity ratio, while the length of the main region of mixing is dependent on velocity ratio only slightly.

***Keywords*—**Air ejector, mixing chamber, CFD.

## I. Introduction

THE article deals with numerical investigation into the flow in a subsonic axi-symmetric air to air ejector with constant area mixing. Quite a number of researchers were concerned with ejectors and a great number of publications have been produced. For example, Sun and Eames [1] named over 100 citations in their overview from 1995. In a review carried out by Bonnington and King [2], 413 references dating prior 1976 were cited. Porter and Squyers [3] compiled a list of more than 1600 references relating to ejector theory and performances.

First methods of ejector design were based on experience. The first analysis of mixing was made by Keenan and Neumann [4]. They consider only the simplest form of ejector, a constant area mixing chamber without diffuser. They calculated the performance of an ejector using the one-dimensional continuity momentum and energy equations. Although the analysis was simplified, the results were consistent and compared well with experimental results. Later Keenan, Neumann and Lustwerk [5] in a follow up to their earlier work, considered mixing at constant pressure. This work produced the first comprehensive theoretical and experimental analysis of the ejector problem, and is the basis of much of what has taken place since. The constant pressure design method is used in the majority of ejector applications, and has caused the most problems for researchers. The main reason for this is the complex nature of the flow structure in the constant pressure mixing section. Also the determination of the mixing chamber geometry to ensure constant pressure mixing and best mixing is problematic.

Only few authors were concerned with optimization of ejectors. Dvořák in work [6] optimized an ejector with the help of Fluent and verified a manufactured ejector experimentally. The ejector was optimized by using turbulence model realizable k-ε with enhanced wall treatment. Model realizable k-ε seemed to be the most suitable for axi-symmetric mixing problems according the results in work of Dvořák [7] also many researches use it, e.g. Rusly, Aye, Charters and Ooi [8], while e.g. Bartosiewicz, Aidoun, Desevaux and Mercadier used turbulence model SST k-ω to simulate the flow in supersonic ejectors in work [9]. Šimák [10] studied numerically flow in a two-dimensional supersonic ejector by several turbulence models and found that turbulence model k-ω is sufficient to capture all important information about the flow. However, it was found in work [6] that all numerical results for various turbulence models varied as compared with experiments.

This study follows work made by Dvořák et al. [11] in which PIV and CTA methods were used to investigate flow in cylindrical mixing chamber. Complex experimental data of four various ejector regimes were obtained and velocity contours and vectors for them were presented. The aim of this study is to analyze the flow in cylindrical mixing chamber.

## II. Methods

### A. Dimensions of the Ejector

The dimensions of the configuration of the nozzle and the mixing chamber are in Fig. 1. For numerical investigation, the ejector had the same dimensions. We used primary nozzle with diameter of $d = 19.2$ (mm) and mixing chamber of diameter $D = 40$ (mm), i.e. the inlet area ratio of nozzles was $\mu = A_1/A_2 = 0.3$. The length of the mixing chamber was $L = 9D = 360$ (mm), the diffuser had divergence angle of 6° and enlargement ratio of the diffuser was $\mu_D = A_4/A_3 = 3.15$.

### B. Numerical Investigation

For numerical calculation we used commercial software Ansys - Fluent 14. On the base of knowledge obtained in works [6] and [7], we used turbulence model realizable k-ε with enhanced wall treatment. This turbulence model is suitable for axi-symmetric problems and proved the best convergence for this kind of problem. The model was two-dimensional and had the same geometry as it is presented in the Fig. 1. The fluid was air considered as ideal gas. Pressure inlets, i.e. total pressures and total temperatures, were used for definition of inlet boundary conditions, pressure outlet, which is back-pressure, was used at the ejector exit. Values of temperatures and pressures on boundaries were taken from experiments in work [11]. The overpressure of primary air

This project was realized with financial support by the Czech Science Foundation, grant no. P101/10/1709.

Vaclav Dvorak is with the Department of Power Engineering Equipment, Faculty of Mechanical Engineering, Technical University of Liberec, Studentska 2, 46007 Liberec, Czech Republic (phone: +420 485 353 479;e-mail: vaclav.dvorak@tul.cz).

stream was $p_{01} - p_{02} = 1000$ (Pa).

*C. Theoretical Approach*

We will compare obtained data with method presented by Tyler and Williamson in work [12]. They divided the mixing processes in the mixing chamber into two regions: The initial region and the main region. They performed a series of experiments for various velocity ratios and cross section ratios.

According them, the momentum equation for constant area mixing chamber has form

$$C_p = 2\beta - 4\bar{f}X - \Delta, \tag{1}$$

where $\bar{f}$ is averaged friction coefficient, $\Delta$ is correction of friction for initial region and $X = x/D$ is relative axial coordinate. $\beta$ is momentum coefficient defined by relation

$$\beta = \frac{A\int_{(A)} v^2 dA}{(\int_{(A)} v \cdot dA)^2} - \beta_T, \tag{2}$$

where $A$ represents cross section, $v$ velocity and $\beta_T \cong 1.02$ is momentum coefficient for fully developed turbulent flow. $C_p$ is static pressure coefficient defined by ratio

$$C_p = \frac{p - p_{12}}{\frac{1}{2}\rho c_3^2}, \tag{3}$$

where $p - p_{12}$ (Pa) is static pressure rise from the beginning of the mixing chamber and the denominator represents dynamic pressure (Pa) of resulting flow. The total pressure coefficient is similarly defined by relationship.

$$C_{p0} = -\frac{p_0 - (p_0)_{12}}{\frac{1}{2}\rho c_3^2} \tag{4}$$

where $(p_0)_{12}$ is total pressure at the entrance of the mixing chamber.

Experimental data was compiled and authors used correlation technic to obtain relation for length of the initial region of mixing

$$l_0 = \frac{C_0}{1-z}\left(\frac{1}{1-\omega}\right)^{n_0}\left(1 - \sqrt{\frac{\mu}{1+\mu}}\right)^{5/3}, \tag{5}$$

where $\omega = v_2/v_1$ is velocity ratio and $\mu = A_1/A_2$ is area ratio of nozzles. Constants obtained by Tyler and Williamson in work [12] by correlation of experimental data are $C_0 = 4.2$ and $n_0 = 1$.

## III. Results and Discussion

Results for ejector mode $\Gamma = m_2/m_1 = 0$ and for velocity ratio $\omega = 0$ are plotted in Fig. 2. It is therefore the mode with zero secondary mass flow rate $m_2 = 0$ and with very high back pressure. As it is seen from contours of axial velocity $c_x$, a separation zone with reversal flow occurred, see gray area.

As it will be shown later, the transition between the initial and main regions is usually in the place, where the shear layer interferes with the wall of the mixing chamber, respectively, with the boundary layer on it. It seems in Fig. 2 that it is not valid for regimes with reversal flows.

Similarly, the transition point is unclear when comparing contours of turbulent kinetic energy $k$ and dissipation $\varepsilon$. As will be shown on the contours of radial velocity $c_r$, the transition can be most easily identified as a place where the radial velocity changes its direction, i.e. $c_r = 0$.

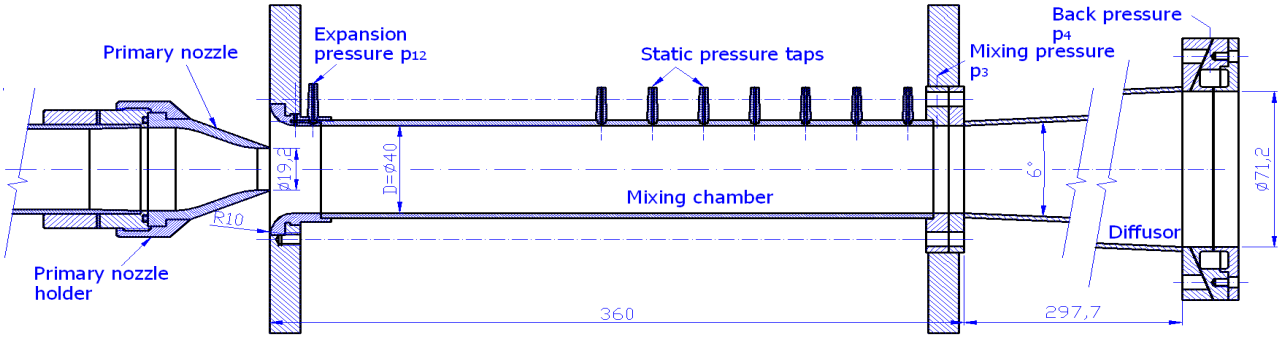


Fig. 1 Dimensions of ejector parts and positions of static pressure taps of the air ejector, investigated experimentally by PIV and CTA methods by Dvořák et al. [11]

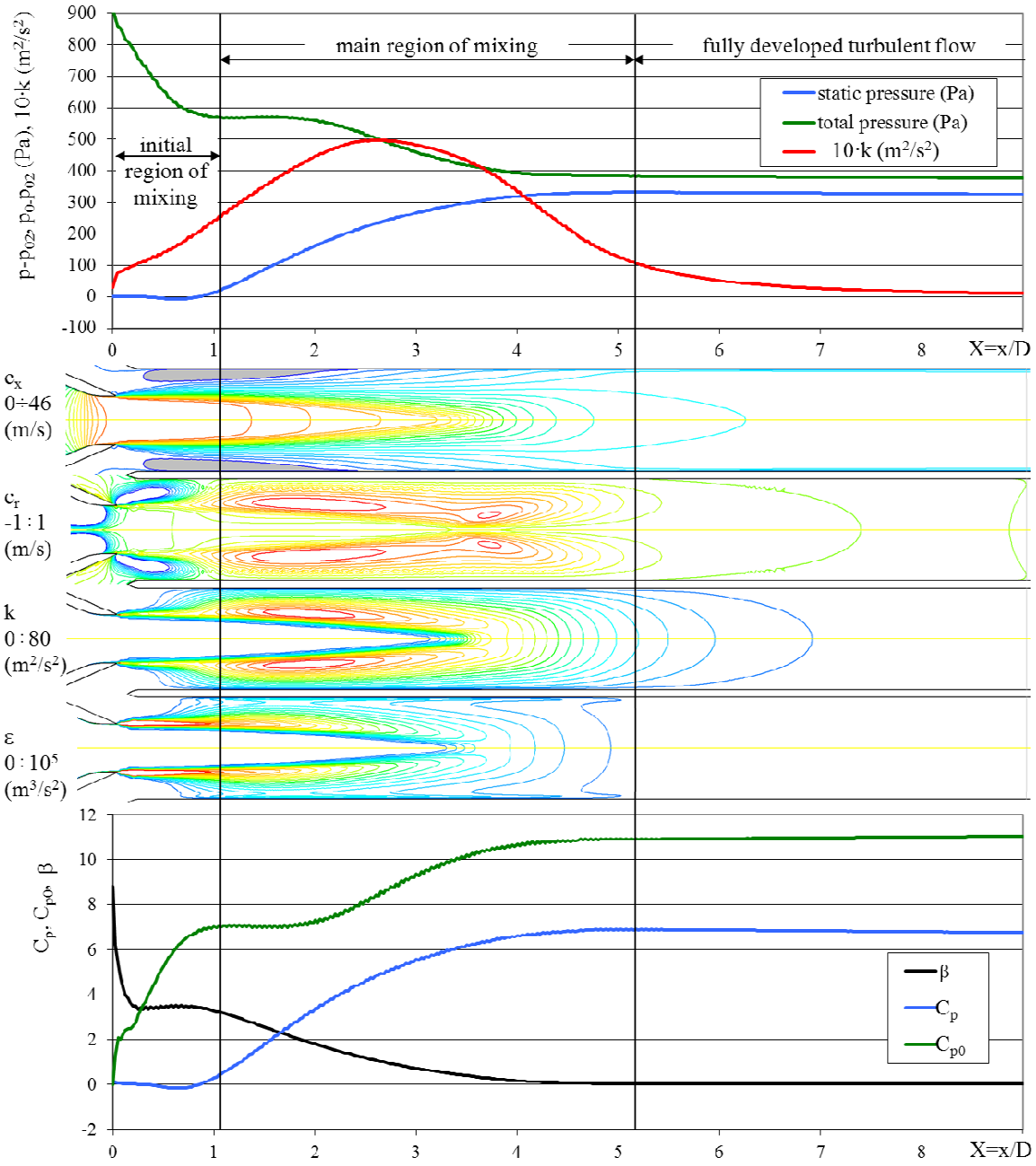


Fig. 2 Ejector mode with ejection ratio $\Gamma = m_2 / m_1 = 0$ and velocity ratio $\omega = 0$. Contours of axial velocity $c_x$, radial velocity $c_r$, turbulent kinetic energy $k$, turbulent dissipation $\varepsilon$, courses of static pressure, total pressure, turbulent kinetic energy, momentum coefficient $\beta$, static pressure coefficient $C_p$ and total pressure coefficient $C_{p0}$

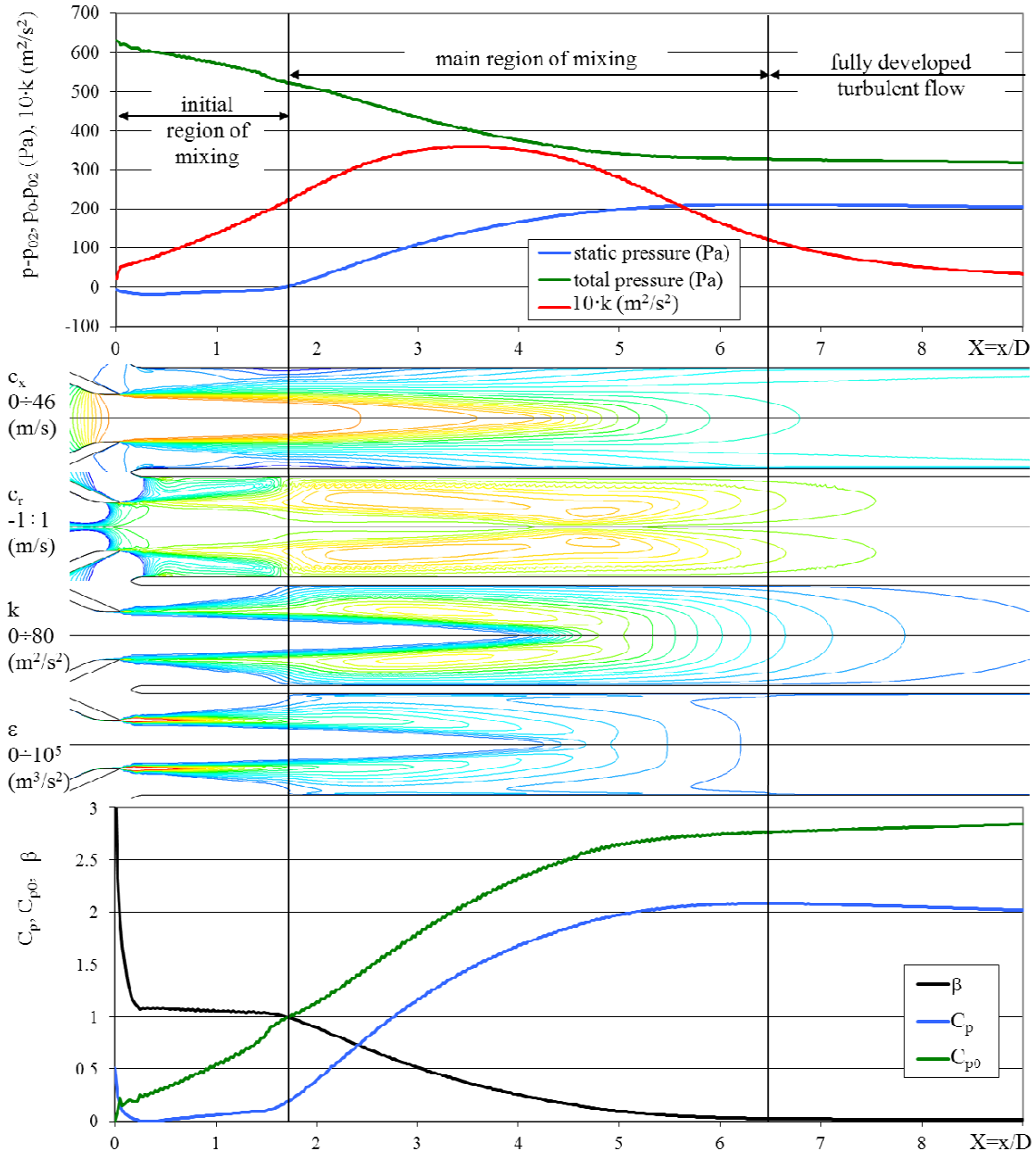


Fig. 3 Ejector mode with ejection ratio $\Gamma = m_2 / m_1 = 0.5$ and velocity ratio $\omega = 0.15$. Contours of axial velocity $c_x$, radial velocity $c_r$, turbulent kinetic energy $k$, turbulent dissipation $\varepsilon$, courses of static pressure, total pressure, turbulent kinetic energy, momentum coefficient $\beta$, static pressure coefficient $C_p$ and total pressure coefficient $C_{p0}$

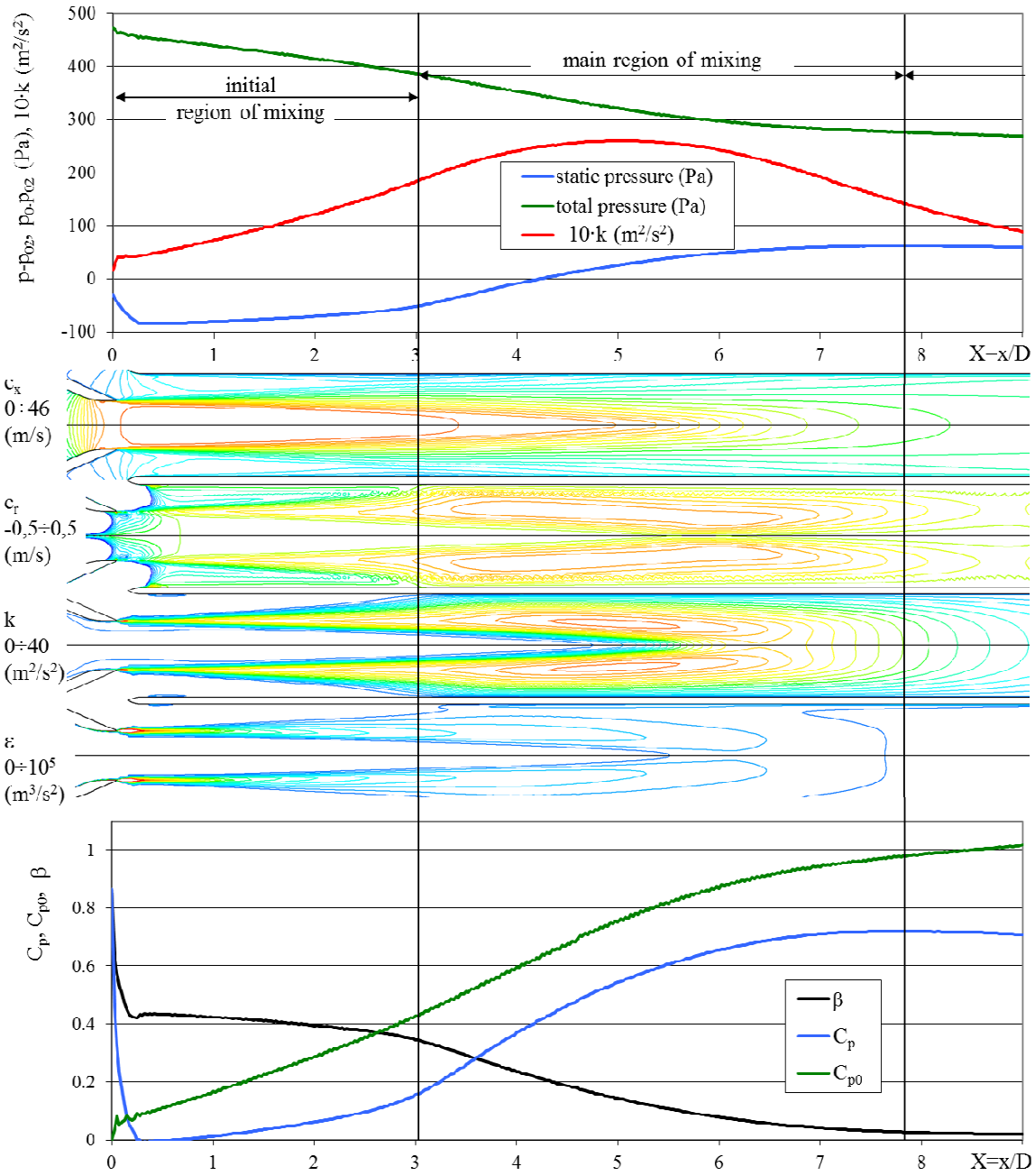


Fig. 4 Ejector mode with ejection ratio $\Gamma = m_2 / m_1 = 1$ and velocity ratio $\omega = 0.3$. Contours of axial velocity $c_x$, radial velocity $c_r$, turbulent kinetic energy $k$, turbulent dissipation $\varepsilon$, courses of static pressure, total pressure, turbulent kinetic energy, momentum coefficient $\beta$, static pressure coefficient $C_p$ and total pressure coefficient $C_{p0}$

The length of the initial mixing region for this mode is $l_0 = 0.9 \cdot D$ and the length of the mixing zone is $l_m = 4.5 \cdot D$. The end of the main region is considered in the point of maximal static pressure. In the top of Fig. 2, static pressure distribution on the mixing chamber wall $p - p_{02}$, total pressure $p_0 - p_{02}$ and kinetic energy $k$, which are evaluated as mass averaged values, are plotted in the diagram. The course of total pressure is affected by the reversal flow for this mode. For other modes, the course of the total pressure fall is more monotonic. The existence of reverse flow does not affect the course of the static pressure. After the maximal static pressure, i.e. after the finished mixing, the static and the total pressure are decreasing similarly. It is caused by fully

developed velocity profile. The maximal kinetic energy is attained at approximately 2/5 of the main region length.

Curves of momentum coefficient $\beta$, static pressure coefficient $C_p$ and total pressure coefficient $C_{p0}$ are plotted in the bottom of Fig. 2. For this mode, the value $C_{p0} = 10.9$ is reached at the mixing chamber outlet.

Results for mode with ejection ratio $\Gamma = 0.5$ and velocity ratio $\omega = 0.15$ are plotted in Fig. 3. In this mode, the reverse flow was absent and the transition between the initial and the main region can be well evaluated. Again, the easiest and most precisely on contours of the radial velocity at the point, where $c_r = 0$, but also on the contours of turbulent kinetic energy $k$ and dissipation $\varepsilon$, from which it is clear that the transition point is at the same point, where the shear layer meets the mixing chamber wall. It is obvious, from axial velocity contours, that the transition caused extension of the boundary layer. The length of the initial mixing region for this mode is $l_0 = 1.6 \cdot D$ and the length of the main mixing zone is $l_m = 4.8 \cdot D$.

It will be shown in the other modes, the length of the initial mixing region depends more on velocity ratio than the length of the main region. The maximum of turbulent kinetic energy is again in approximately 2/5 of the main mixing region. The decrease of the total pressure is much more gradual than in previous case, slightly higher losses are in the main mixing region. The resulting decrease of the total pressure is at the end of the mixing is $C_{p0} = 2.75$.

Similar remarks can be done in the next mode in Fig. 4 for mode with ejection ratio $\Gamma = 1$ and velocity ratio $\omega = 0.3$, again without return flow. Mixing is already quite slow in this case, the length of the initial region of mixing increased to $l_0 = 3 \cdot D$ and the length of the main mixing zone is $l_m = 5 \cdot D$.

The last investigated mode was for ejection ratio $\Gamma = 1.5$ and velocity ratio $\omega = 0.45$. For this mode, which is not presented in the article, the length of the mixing chamber was already insufficient, so only the length of the initial region of mixing could be evaluated as $l_0 = 4.2 \cdot D$. The end of mixing occurred after the mixing chamber. The values obtained for the various modes are plotted in Table I.

TABLE I
EVALUATION OF NUMERICAL RESULTS FOR VARIOUS MODES

| Ejection ratio $\Gamma$ | 0 | 0.5 | 1 | 1.5 |
|---|---|---|---|---|
| Velocity ratio $\omega$ | 0 | 0.5 | 0.3 | 0.45 |
| Length of the initial region of mixing $l_0/D$ | 0.9 | 1.65 | 2.8 | 4.625 |
| Length of main region of mixing $l_h/D$ | 4.5 | 4.8 | 5 | - |
| Static pressure rise $C_p$ | 6.8 | 2.1 | 0.7 | $\geq 0.2$ |
| Total pressure drop $C_{p0}$ | 10.9 | 2.75 | 0.98 | $\geq 0.5$ |

## IV. DISCUSSION

Let us now look in more detail at each of the mixing region in general. The initial mixing region begins at the trailing edge of the primary nozzle. It is the area in which there is an unaffected secondary air flow and its end is defined as a place in which unaffected secondary air flow vanishes, i.e., meet the two shear layers that enclose driven flow: free shear layer (mixing layer) between the primary and secondary flows from one side and the boundary layer on the mixing chamber wall from the other side.

For the initial mixing region, very small increase in static pressure is typical. In some cases, for high velocity ratios, the static pressure even falls due to friction losses. Sometimes this case can be considered as a free jet flow. Small change in static pressure is of course due to a small change in momentum. It can be shown that the decrease of momentum due to change of the velocity profile between the beginning of the mixing chamber and the end of initial mixing region is very small.

It turns out, however, that the pressure increase in the initial mixing zone affects the flow in the mixing chamber rather negatively. The increase in pressure caused deceleration of the secondary air flow, see contours of $c_x$, and extension of the boundary layer. As a results, the secondary air flow is pushed to the mixing layer, see the contours of $c_r$.

The aim of the mixing is but opposite, i.e., the acceleration of the secondary stream and mass transfer in the direction to the secondary stream. The main disadvantage of the constant area mixing chamber and the reason why it cannot be effective enough are: At the beginning, the secondary stream is slowed down and the fluid is displaced toward the primary stream, and only in the main region of mixing the secondary stream is accelerated and energy begins to move into the secondary stream.

Although the change of momentum in the initial region of mixing is small, the total pressure drops by almost the same intensity as in the main region of mixing.

Turbulent kinetic energy increases from the beginning of the mixing chamber as the mixing layer expands. The length of the initial region of mixing is obviously very strongly dependent on the velocity ratio.

Once the boundary layer on the mixing chamber wall and the mixing layer meet, the momentum falls and the static pressure rises faster. At this point, there is the highest deceleration of fluid in the boundary layer, which is not yet accelerated by faster fluid from the mixing layer. The modes with small velocity ratios, when the secondary stream is slow and the pressure rise is extreme, a flow separation can occur at this point.

The transition between the initial and main area is very sharp. From this point, the momentum coefficient decreases rapidly and it is the place of the largest gradient of the static pressure. In the main region of mixing there is no longer unaffected secondary stream, and if the core of the primary

stream has disappeared, the mixing layer occupies the entire cross section of the mixing chamber.

The turbulent kinetic energy increases and reaches its maximum at approximately 2/5 of the length of the main region of mixing. Obviously, the length of the main mixing zone is only little dependent on the velocity ratio, the main effect is may be caused only by the ratio of cross sections.

End of the main region of mixing is considered by many researchers as the point of maximum static pressure. Let's look at this in more detail cross section. According to Tyler and Williams [12] the end of mixing is at the point where momentum coefficient falls to normal value of fully developed turbulent flow, but the exact value is not strict, and the size is different for each Reynolds number. From the analysis of the numerical calculations, the point of the maximal static pressure corresponds approximately to the point, where the turbulent kinetic energy has its maximal value in the centre of cross section of the mixing chamber, while the maximal values are bound to the mixing layer in the beginning of mixing. After this point, the dissipation decreases and the total pressure fall is caused mainly by friction losses.

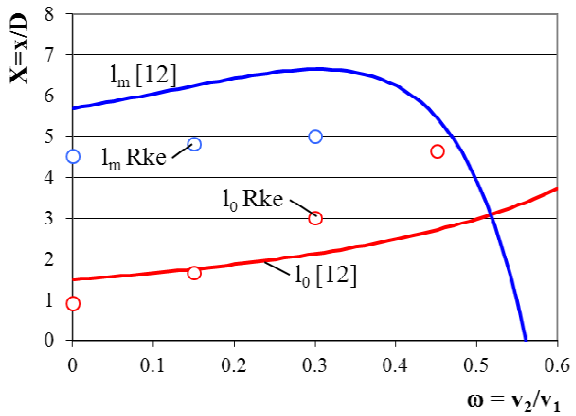


Fig. 5 The lengths of initial mixing region $l_0$ and main mixing region $l_m$ according [12] and obtained by numerical calculation with turbulence model realizable *k*-ε (Rke)

As shown in Fig. 5, where is a prediction of the length of the main region of mixing according to [12], the theoretical and numerical values does not agree very well. The results do not correspond to the values calculated using the model of turbulence Realizable k-ε nor measured mainly for higher velocity ratio. There is of course the question of the role of initial conditions of the turbulence, Reynolds number, and more. But it is clear that the method [12] based on empirical data correlation may not apply generally to other ejector configuration than those used in [12]. Determining of the correct coefficients for our case would require similarly large-scale experiments, which made mentioned authors, and also there would be no universal method.

## V. Conclusions

The presence of the initial and the main mixing region were confirmed. In the initial mixing region, an unaffected secondary air stream exists. It starts at the trailing edge of the primary nozzle and the end can be defined as a place in which two shear layers enclosing secondary stream meet: free shear layer (mixing layer) between the primary and secondary streams from one side and the boundary layer on the wall of the mixing chamber from the other side. Very small increase in static pressure associated with a small decrease in momentum is typical for the initial mixing region. The primary stream can be considered as a free stream.

It turns out that the pressure increase in the initial region effects the mixing processes rather negatively. It decelerates the secondary stream and extends the boundary layer, which pushed the secondary stream towards the mixing layer. The mixing is but opposite, i.e. the acceleration of the secondary stream and the mass and momentum in the direction of the secondary stream. Having said that the main disadvantage of the constant area mixing chamber and the reason why it cannot be effective enough: At the beginning of the mixing chamber, the secondary stream is slowed down and the fluid is displaced toward the primary stream. Only in the main mixing region the secondary stream is accelerated and fluid begins to move into the secondary stream.

Although only a small change of momentum occurs in the initial region, the stagnation pressure drops by almost the same intensity as in the main region. Length of initial mixing zone is obviously very strongly dependent on the relative velocity.

Once the mixing layer meets the edge of the boundary layer on the wall of the mixing chamber, the momentum begins to fall faster and also the static pressure rises faster. There is the greatest deceleration of fluid in the boundary layer, which is not yet accelerated by faster fluid from the mixing layer at this point. A flow separation and reversal flow occurs at this point for ejector modes with low velocity ratios.

The transition between the initial and main area is very short. From this point, momentum coefficient decreases rapidly and it is the place of the highest gradient of static pressure. There is no longer unaffected secondary stream in the main region of mixing. If the core of the primary stream has disappeared, the mixing layer occupies the entire cross section of the mixing chamber. Obviously, the length of the main mixing zone is only little dependent on the velocity ratio. According to many researchers, the end of mixing placed in a position of maximal static pressure. It is approximately the point, where the turbulent kinetic energy has its maximal value in the axis of the mixing chamber, while the maximal value is bound to the mixing layer in the beginning of mixing.

## References

[1] D.W. Sun, I.W. Eames, Recent Developments in the Design Theories and Applications of Ejectors – a review, *Journal of the Institute of Energy, 65-79 (1995)*

[2] S.T. Bonnington, A.L. King, Jet Pumps and Ejectors, a State of the Art; Review and bibliography (2nd edn), *BHRA Fluid Eng, Cranfield, Bedford UK (1976)*
[3] J.L. Porter, R.A. Squyers, A Summary/Overview of Ejector Augmentor Theory and Performance, *ATC Report No. R-91100/9CR-47A, Vought Corpn Advanced Technology Cr, Dallas, Texas (1981)*
[4] J.H. Keenan, E.P. Neumann, A Simple Air Ejector, *J Applied Mechanics, Trans ASME 64, A75 - A81 (1942)*
[5] J.H. Keenan, E.P. Neumann, F. Lustwerk, An Investigation of Ejector Design by Analysis and Experiment, *Journal of Applied Mechanics, Trans ASME 72, 299-309 (1950)*
[6] V. Dvořák, Optimized Axi-Symmetric Ejector – Experimental and Numerical Investigation, *Experimental Fluid Mechanics 4 (1), 34-43 (2009)*
[7] V. Dvořák, Numerical Computation of Efficiency Curve of Ejector, *Conference ANSYS, Prague, 149-156 (2007)*
[8] E. Rusly, Lu Aye, W.W.S. Charters, A. Ooi, CFD Analysis of Ejector in a Combined Ejector Cooling System, *International Journal of Refrigeration 28, 1092-1101 (2005)*
[9] Y. Bartosiewicz, Z. Aidoun, P. Desevaux, Y. Mercadier, Numerical and experimental investigations on supersonic ejectors, *International Journal of Heat and Fluid Flow 26, 56-70 (2005)*
[10] J. Šimák, Computation of the Flow and Interaction of Shock Waves in a 2D Supersonic Ejector, *Colloquium Fluid Dynamics 2009, Institute of Thermomechanics AS CR, v.v.i., Prague, Czech Republic, October 21 - 23, 2009*.
[11] V. Dvořák, P. Novotný, P. Dančová, D. Jašíková, PIV and CTA Measurement of Constant Area Mixing in Subsonic Air Ejector, *Experimental Fluid Mechanics 7 (1), 109-114 (2012)*
[12] R. A. Tyler, R. G. Williamson, Confined mixing of coaxial flows, *Aeronautical report LR-602, NRC no. 18831 (Division of Mechanical Engineering, Ottawa, Canada 1980).*